Blockchain Assisted Al-Biruni Earth Radius Optimization with Deep Learning Model for Sustainable Healthcare Disease Detection and Classification

Omar Ahmed Abdulkader[1,*]

[1]Faculty of Computer Studies, Arab Open University, Riyadh, Saudi Arabia
Email: o.abdulkader@arabou.edu.sa

Abstract

The cybersecurity and sustainability concepts involve safeguarding and analyzing sustainable systems, providing a versatile perspective. In the extensive data landscape of sustainable healthcare systems, ensuring diagnostic and security processes poses challenges. Healthcare disease detection using Blockchain (BC) employs BC technology to boost security and precision. This system securely shares and stores patient records through BC, fostering collaboration among researchers and healthcare providers to improve disease detection accuracy. This study designs a new BC-Assisted Al-Biruni Earth Radius Optimization with Deep Learning Model for Sustainable Healthcare Disease Detection and Classification (BAERDL-SHDDC) technique. The BAERDL-SHDDC technique presented utilizes BC to securely store patient data and employs DL models to analyze the data for the disease detection process. For disease detection, the BAERDL-SHDDC technique involves a three-stage process namely Al-Biruni Earth Radius (AER)-based feature selection, ensemble DL classification, and hyperparameter optimization. The hyperparameters of the ensemble DL models with fractals optimizations are optimally selected using an Adadelta optimizer. The stimulation result analysis of the BAERDL-SHDDC approach shows the guaranteeing performance of the BAERDL-SHDDC algorithm over other existing techniques with greater accuracy of 98.45%, 95.22%, and 96.49% under Heart Statlog, Pima Indian Diabetes, and EEG Eyestate databases respectively

Keywords: Cybersecurity; Sustainability; Healthcare diagnosis; Blockchain; Security; Fractals Optimization; Deep learning

1. Introduction

The growth of Information and Communication Technology (ICT) has transformed the world into a novel era, where every requirement is just on single click [1]. The new control systems and technologies had a dynamic role in all walks of human life namely smart homes, industrial automation, healthcare, and smart cities. Of these, healthcare will be a very significant one, which is considered fundamental to human life. In smart healthcare systems, biomedical parameters of patients like Electrocardiograph (ECG), pulse rate, blood sugar level [2], Electroencephalogram (EEG), and other crucial biomedical signs are diagnosed and checked by implanting sensing and tracking tools in the human body. Electronic Health Records (HER) offer a useful and substantial dataset to diagnose and identify several diseases and grant one type of judgment for managing health disputes. Intellectual methodologies like Cloud-Assisted approaches [3], Deep Learning (DL), and Machine Learning (ML) have attained popularity for the prevention and detection of diseases in recent times. ML and DL were encountering certain insufficiencies in the context of flexibility, scalability, availability, and security [4]. So, a few cloud-related healthcare data-sharing methods were used earlier to provide security, scalability, flexibility, and economic details using data encryption and operation depersonalization. Due to concerns about the privacy and sensitivity of user's data [5], users were reluctant to transmit their data to the cloud. To solve the issues in previous methods there was a necessity for an interoperable secure mechanism, and to formulate a scalable and efficient structure that manages every problem mentioned above.

DOI: https://doi.org/10.54216/JCIM.150209
Received: May 05, 2024 Revised: July 10, 2024 Accepted: October 22, 2024

At present, BC Healthcare is the application that is mostly leveraged to maintain healthcare data, safe and secure. Security has become a main challenge in the healthcare industry [6]. But BC technology can decentralize logs, and keep transparent, incorruptible, and information regarding all patients. This characteristic makes it technology suitable for security applications. On top of that, BC can be isolated and obvious about the person individuality with complicated and secure codes and could secure the sensitivity of medical data too. While the technology was decentralized [7], it facilitates doctors, patients, and medical service sources for sharing the same data among themselves rapidly and securely. The main difficulty, while managing these healthcare data, is to assure data privacy from various kinds of cyberattacks like unauthorized access and tampering [8]. BC has safe the location of digital ledger that can be organized to record communications in finance and other fields, wherever the protection of historic records of e-transactions was crucial. BC is the key technology in Bitcoin, a type of cryptocurrency. Bitcoin was created after the economic crisis of 2009, as a substitute for classical currency [9]. The important causes behind the initiation of technology was the failures of centralized banks based on conserving financial reports. Financial organizations for a notable period, have differentiated the necessity for a dispersed decision-making approach [10]. But, these techniques are not applied, until the development of crypto-currency fuelled by the technology of BC.

This study introduces a novel BC-Assisted Al-Biruni Earth Radius Optimization with Deep Learning Model for Sustainable Healthcare Disease Detection and Classification (BAERDL-SHDDC) technique. The aim of the BAERDL-SHDDC model is to exploit BC for secure patient data management and disease diagnosis process. In addition, the BAERDL-SHDDC technique involves a three-stage process namely Al-Biruni Earth Radius (AER)-based feature selection, ensemble DL classification, and Adadelta-based parameter optimization. The hyperparameters of the ensemble DL models are optimally selected by the usage of an Adadelta optimizer. The performance validation of the BAERDL-SHDDC model can be examined on three medical datasets.

2. Related Works

Veeramakali et al. [11] developed the best DL-associated Secure BC (ODLSB) based intellectual Internet of Things (IoT) and health care diagnosis method. This presented method contains the Orthogonal Particle Swarm Optimizer (OPSO) method for the safe sharing of healthcare images. Along with this, with the Neighbourhood Indexing Sequence (NIS) approach, the hash value encrypting process takes place. Lastly, the Optimum Deep Neural Networks (ODNNs) was implemented as a classifier method for diagnosing diseases. Neelakandan et al. [12] propose an innovative BC with a DL-allowed Secure Medical Data Transmission and Diagnosis (BDL-SMDTD) algorithm. The BDL-SMDTD approach intended to safely transfer medical images and identify illnesses with a greater recognition rate. Mainly, Mayfly Optimizer (MFO) and Elliptic Curve Cryptography (ECC), together known as MFO-ECC methodology were employed for the process of image encryption in which the best ECC keys were made with the MFO approach.

Nguyen et al. [13] devised a safe Intrusion Detection (ID) with BC-based data communication with a classifier method for Cyber-Physical Systems (CPS) in the medical field. This method performed data acquisition through sensor devices and ID happens with the help of the Deep Belief Network (DBN) approach. As well, the BC technology can be implemented for secure data transmission to the server, which implements the ResNet-based classifier for identifying the disease. Chen et al. [14] devised a BC-based diabetes disease identification structure that offers an initial identification of this disease through several ML classifier techniques and maintains the EHRs of patients securely. This structure for sharing EHRs integrates symptom-related disease forecasting, BC, and the Interplanetary File System (IPFS), collecting users' health records through wearable sensor devices.

In [15], FIDChain IDS was presented through a lightweight Artificial Neural Network (ANN) in a Federated Learning (FL) way to assure healthcare data confidentiality protection with the advancement of BC that offers a disseminated ledger to aggregate local weights and broadcast the upgraded global weights after averaging that thwarts murdering assaults and offers and complete transparency stability over the dispersed system with insignificant overheads. Smahi et al. [16] presented a BC-based privacy-maintaining SVM classifier over a vertically divided IoMT dataset for the Clinical Decision Support (CDS) mechanism. Both the global classification model and local building training run on certifiable and isolated smart contracts instead of depending on unreliable third persons. In [17], the author a DL-related data analytics and privacy protection mechanism for IoT-based health care. Finally, raw data is collected, and the users' privacy data is in a privacy isolation zone.

3. The Proposed Model

In this article, we have proposed a new BAERDL-SHDDC technique for sustainable and secure healthcare management. The proposed BAERDL-SHDDC technique exploited BC technology for secure patient data management and DL models to examine the data for the disease detection process. The BAERDL-SHDDC

DOI: https://doi.org/10.54216/JCIM.150209
Received: May 05, 2024 Revised: July 10, 2024 Accepted: October 22, 2024

technique offered improved security for patient data with enhanced disease classification performance via feature selection and ensemble process. Fig. 1 demonstrates the complete working flow of the BAERDL-SHDDC model.

A. Hyperledger BC-based Secure Data Management

Hyperledger is a management which renders many open-source BC and hyper ledger fabric is among them [18]. Also, the study aims to provide a decentralized environment. It includes committing order, peer, Certificate Authority (CA), endorser peer, and client. Moreover, the component connects using a channel that is used to enable the transaction secretly and privately, which splits various fields of application. The committing peer was accountable to proceed with the chain transmitted by the channel created in the mechanism. Therefore, they save different BCs, for the generated channel. This scalability and privacy were offered by the 'individual chain per channel'. Consequently, ordering a peer implemented on a specific chain should authorize whether the transaction is added to the committing peer.

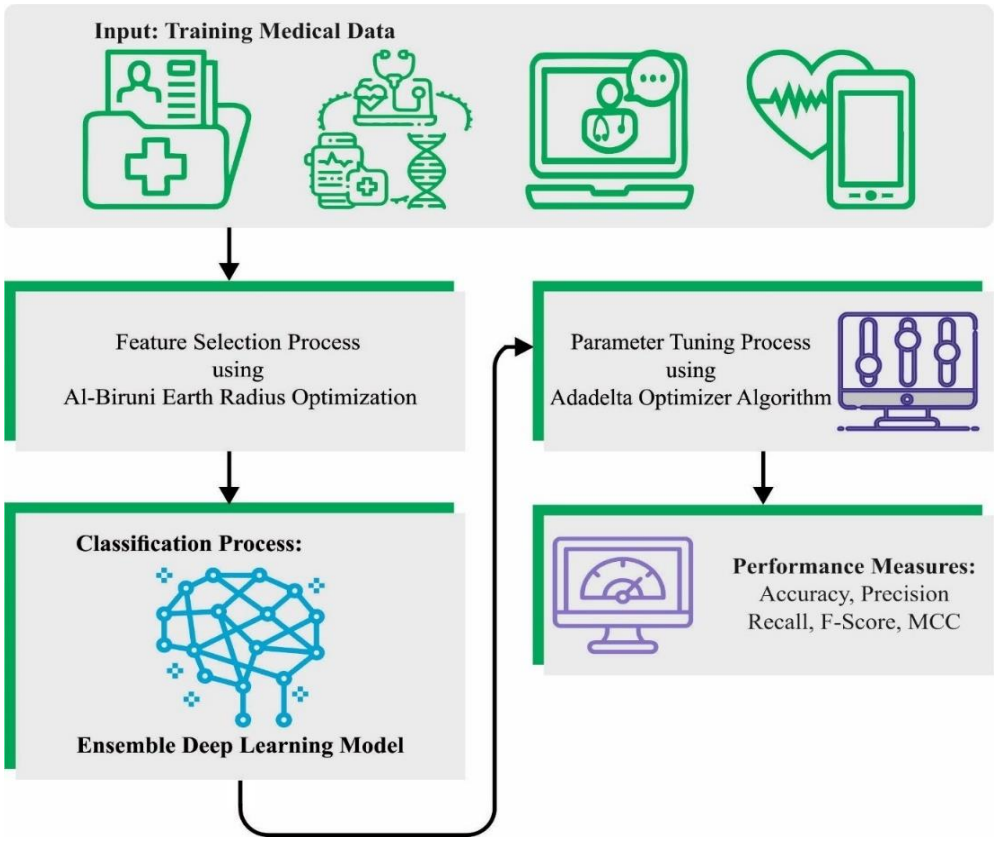

Figure 1. Overall flow of BAERDL-SHDDC approach

The fabric CA is accountable for two processes. At first, to guarantee different components (smart contracts or user) to utilize the system that can be specified and then, validate the component and authorize to employ it for a specific function (i.e., performing transactions) or accessing other components which leads to authorization. Gathering peer executes two processes namely it attains client transaction and organizes the transaction to monitor the reliability of the BC. Authorizing peers is accountable for two processes. Firstly, gather transaction from the user, and then analyzed by the smart contract mechanism from which the transaction has many relevant rules that need to be followed. It is pointed out that a user can often visit a similar medical institution, and the BC saves a single visit. The BC for every medical institution (known as local BC) stores EHR related to the individual. To locate the BC, it is deliberated that the medical organization retains the minimum architecture needed to carry out the Hyperledger network. A smart contract is an application of chain code in Hyperledger Fabric.

A chain code can be widely utilized to perform network-agreed business logic. Fig. 2 defines the structure of BC. When the chain code is created, the resultant state becomes private to that chain code and unreachable by another chain code. If the user has the necessary authorization, it is possible to call another chain code. Concerning chain codes, it is useful to consider 2 dissimilar categories: chain code for the system of application-specific code system chain code was usually responsible for handling system-related transactions, like lifecycle management and policy configuration.

DOI: https://doi.org/10.54216/JCIM.150209
Received: May 05, 2024 Revised: July 10, 2024 Accepted: October 22, 2024

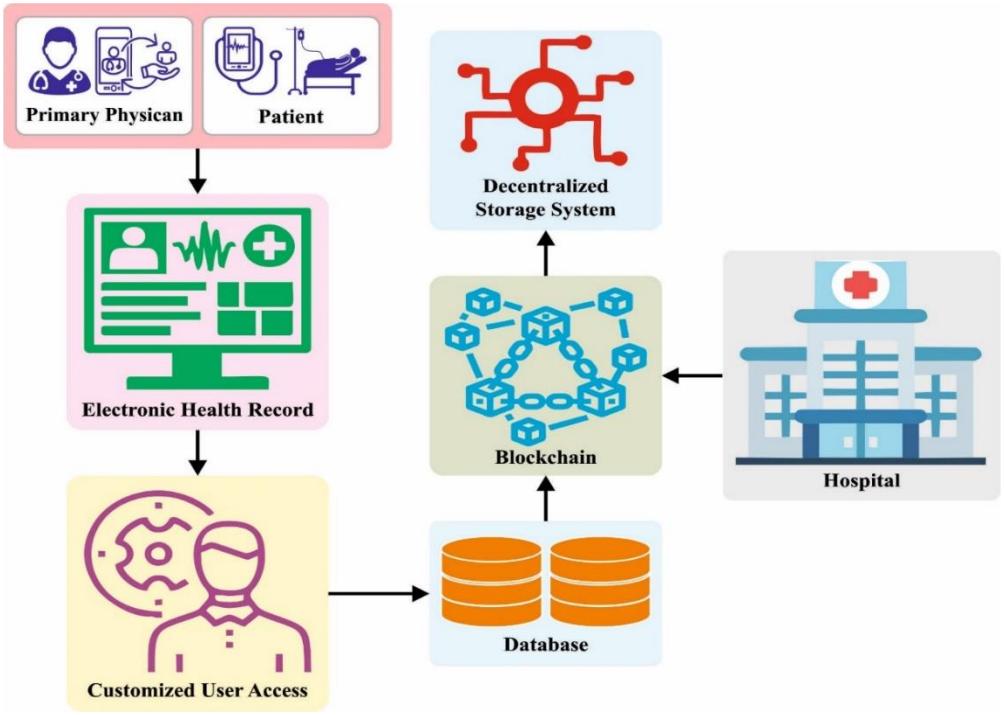

Figure 2. Structure of BC

The application chain code was in charge of keeping the application states like digital properties or random entries of data on the ledger. The medical professional secured the private permissioned network for registered stakeholders. Every person works with further security utilizing a Virtual Private Network (VPN) connection for accessing the registration mechanism. During registration, patients give registration data like contact information, name, social security number, and address. In addition, all previously mentioned will be registered with the medical professional: main physician, laboratory, hospital, researcher, insurance, and pharmacy. The public healthcare specialist verifies the record and provides chain code addresses after they have finalized the registration procedure. Every transaction on the network is completed, and now, each party has completed the registration process.

B. Feature Selection using AER Algorithm

The earth radius computation is depending on the Al-Biruni technique which forms the backbone of the AER optimization approach [19]. The objective of the optimization algorithm is to find the optimum solution within specified constraints. Every individual in the population is characterized by tt$S = S_1, S_2, \ldots S_d \in R$, where S_d represents a size of the searching region and d denotes the size of the feature or parameter being improved. It is suggested that success up to a certain limit can be evaluated by the fitness function F. With this stage of optimization technique, the population might be examined for the fitness-maximizing vector S^*. Several factors should be determined before AER can begin optimizing, they are the population size, fitness function, dimension, the number of solutions, and the minimal and maximal allowed solution sizes. Exploitation and Exploration processes create the basis of the AER technique as discussed below:

Exploration Operation: This phase can be accountable for finding potential regions of the search range and breaks by local optima directed the optimum solutions.

Move to the optimum solution: the individual explorer will search the instant area around its existing position for possibly a novel exploration site. For achieving this, an iteration method is used to find a more optimum option from the many available choices neighboring AER analysis applies the subsequent formula to achieve these goals:

$$r = h\frac{cos(x)}{1 - cos(x)} \quad (1)$$

$$D = r_1(S(t) - 1) \quad (2)$$

$$S(t+1) = S(t) + D(2r_2 - 1) \quad (3)$$

DOI: https://doi.org/10.54216/JCIM.150209
Received: May 05, 2024 Revised: July 10, 2024 Accepted: October 22, 2024

Where $0 < \chi \leq 180$, h represents the randomly selected numAER within [0,2], r_1 and r_2 denote the coefficient vector whose value is evaluated using Eq. (1), $S(t)$ indicates the solution vector on t iteration, and D signifies circle diameters while searching agent identifies possible regions.

Exploitation Operation: This phase is answerable for enhancing the existing solutions. The AER estimates the fitness of every participant once the cycle ends, and awards those with a better score. The AER applies two different approaches to accomplish the objective of exploitation, both of which are discussed below:

Moving in the direction of optimum solution: The subsequent formula is used for moving towards the better solution.

$$S(t+1) = r^2(S(t) + D) \tag{4}$$

$$D = r_3\big(L(t) - S(t)\big) \tag{5}$$

Where r_3 denotes the random vector evaluated by Eq. (2) which controls the movement step toward the better solution, $S(t)$ denotes the vector of solution at iteration t, $L(t)$ indicates the better solution vectors, and D indicates the vector of distance.

Finding the region around a better solution: In general, the area around the optimum responses provides the utmost possible for success (leader). Consequently, few people hunt for a way to improve the situation by exploring alternatives that are approximately equivalent to the optimum one. AER employs the subsequent equation to perform the abovementioned procedure.

$$S'(t+1) = r(S^*(t) + k) \tag{6}$$

$$k = 1 + \frac{2 \times t^2}{\mathrm{Max}_{iter}^2} \tag{7}$$

In Eq. (6) and (7), a better solution can be attained by $S^*(t)$ that is chosen afterward comparing $S(t+1)$ and $S'(t+1)$. If the optimum fitness wasn't changed in the last two iterations, then the subsequent formula is used for mutating the solution.

$$S(t+1) = k * z^2 - h\frac{\cos(x)}{1 - \cos(x)} \tag{8}$$

In Eq. (8), z represents the arbitrary numAER in [0,1] and t represents iteration count.

Selection of the better solution: the AER chooses the better one to ensure that the solution is of superior quality to apply within the following cycle. Where the elitism method is the best performing, it might lead multimodal function to converge earlier. The AER is capable of delivering cutting-edge exploration abilities by capturing a transformative technique and scanning the region surrounding the explorer. Also, the AER can be capable of staving off convergence with its powerful exploration abilities. Firstly, the parameters like iteration count, population size, and mutation frequency are inputted into the AER. Then, the AER allocates individuals to the exploitation or exploration group. The AER technique dynamically adjusts the size of every group all over the iteration method to locate the better solution. To complete their missions, each group used two strategies. The AER guarantees comprehensive exploration and diversity by rearranging the order of response among repetition. In single iteration, a solution might be the part of exploitation groups, while in the next, it might be the part of exploration group. The leader will not be deposed due to the exclusive nature of AER.

The fitness function (FF) of the AER algorithm measured the classification precision and particular features. It maximized the classification accuracy and minimized the set size of the particular features. Later, the FF is leveraged to assess separate solutions, as specified in Eq. (17).

$$Fitness = \alpha * ErrorRate + (1 - \alpha) * \frac{\#SF}{\#All\_F} \tag{9}$$

Where ErrorRate indicates the classification rate of error by using the particular attributes. ErrorRate was calculated as the percentage of an improper classifier to several classifications done, indicated as a value in-between (0,1). $\#All\_F$ is the overall amount of features within the original dataset and $\#SF$ is the amount of selective attributes. α is needed to manage the significance of classifier quality and subset length. In this experiment, α is fixed to 0.9.

DOI: https://doi.org/10.54216/JCIM.150209
Received: May 05, 2024 Revised: July 10, 2024 Accepted: October 22, 2024

C. Weighted Voting-based Ensemble Classification

GRU and LSTM as an ensemble of the weighted voting classifier are applied for the classification method. The DL technique is integrated, and the greatest resultant was chosen by the weight voting process. Whereas n number of classes and base classifier as D for voting, the predictive class c_k of weight votings for each k instance is expressed as follows:

$$c_k = \arg\max_j \sum_{i=1}^{D} (\Delta_{ji} \times w_i) \tag{10}$$

In Eq. (10), Δ_{ji} specifies binary variable. When $i\text{-}th$ base classifier categorized the k samples into jth classes, then $\Delta_{ji} = 1$, or else, $\Delta_{ji} = 0$. w_i demonstrates the weights of $i\text{-}th$ base classifier:

$$Acc = \frac{\sum_k \{1 | c_k \text{is the true class of instance } k\}}{\text{Size of test instances}} \times 100\% \tag{11}$$

i. GRU Model

GRU is an LSTM model that obtains the RNN benefits: it effectively models long dependency datasets and automatically learns features [20]. It is exploited for the prediction of short-term traffic. Impulsively, forget and input gates were incorporated as reset gates in GRU that defines how to integrate newly inputted data within the prior time. Other gate in GRU is an update gate; it describes the dataset from the prior time kept to the present time. Thus, GRU was single gate less than LSTM. It creates the GRU model have fewer variables and rapid training velocity as well as necessitates fewer datasets to effectively simplify the model:

$$z_n = \sigma f(W_z \cdot [h_{n-1}, x_n]) \tag{12}$$

$$r_n = \sigma f(W_r \cdot [h_{n-1}, x_n]) \tag{13}$$

$$\overline{h}_n = \tanh(W \cdot [r * h_{n-1}, x_n]) \tag{14}$$

$$h_n = (1 - z_n) * h_{n-1} + z_n * \overline{h} \tag{15}$$

Eqs. (12) & (13) demonstrate how r_n, z_nreset, and update gates are assessed. W_z refers to the weight of z_n, 0 signifies the sigmoid function, $and\ W_r$ symbolizes the weight of r_n. A large value of z_n represents that data was conserved through the existing cell r_n recommends that while the value is equal to 0, data from the previous cell was eliminated. Eqs. (14) & (15) illustrate the approximation of h_n and $\overline{h}$ last and pending output of GRU-NN. W symbolizes the weight of z_n, h_{n-1} represents the output from the earlier cell, and tanh indicates the hyperbolic tangent function. $\overline{h}_n$ can be gained by multiplying h_{n-1} of the previous cell using r_n and x_n, multiplying by W and tanh. h_n represents the sum of dual vector.

ii. LSTM Model

The RNN method is most commonly used for analyzing and forecasting time sequence datasets. RNN frequently undergoes the problem of vanishing gradients [21]. Therefore, it is difficult to remember the prior datasets such as the long dependence problems. To resolve this problem, the LSTM is presented and employs a gate-controlling technique for modifying data flow and constantly defines the amount of received data, which can be retained from every time step.

The structure of the LSTM module is composed of 3 control gates (output, forget, and input gates) and a storing unit. x_z and h_z correspond to the input and hidden state of time z. f_z, i_z, and o_z define the output, input, and forget gates. $\vec{C}_z$ shows the candidate data to the input.

$$f_z = \sigma f\left(W_f \cdot [h_{z-1}, x_z] + b_f\right) \tag{16}$$

$$i_z = \sigma(W_i \cdot [h_{z-1}, x_z] + b_i) \tag{17}$$

$$o_z = \sigma(W_o \cdot [h_{z-1}, x_z] + b_o) \tag{18}$$

$$\tilde{C} = \tanh(W_C \cdot [h_{z-1}, x_z] + b_C) \tag{19}$$

$$C_z = f_z \cdot C_{z-1} + i_t \cdot \tilde{C} \tag{20}$$

$$h_z = o_z \cdot \tanh(C_z) \tag{21}$$

DOI: https://doi.org/10.54216/JCIM.150209
Received: May 05, 2024 Revised: July 10, 2024 Accepted: October 22, 2024

Whereh_{z-1} implies the resulting memory module from the prior time interval z-1, W_f, W_i, W_o, and W_c b_f, b_i, b_o, and b_c correspondingly represent the weighted matrix and bias vectors of forget, input, output, and update states.= and x^z signifies time series data of the present time interval z.

iii. Adadelta-based Hyperparameter Tuning

In this study, the hyperparameters of the DL models involved in the ensembling process take place using the Adadelta optimizer. Adadelta refers to an adaptive learning rate optimizer technique for gradient descent-based optimization. It was presented in 2012 and was an extension of Adagrad [22], which even adapted the learning rate for all parameters. Adadelta addressed certain constraints of Adagrad through a running average of squared gradient as an alternative to the historical gradient to upgrade the learning rate. This permits Adadelta to learn even if the gradient is small and the learning rate would be very small. Adadelta was well-suited for issues where the cost function was changing over time and the optimal learning rate was changing. It is utilized in DL applications, particularly in LSTM networks and Recurrent Neural Networks (RNN).

4. Results and Discussion

In this section, the performance of the BAERDL-SHDDC approach can be validated by utilizing three medical datasets [23-26] such as the EEG Eyestate, Heart Statlog, and Pima Indian Diabetes, and are chosen for their diversity in medical conditions and comprehensive attributes, providing a robust investigation of the performance of the BAERDL-SHDDC approach across different healthcare scenarios. An elaborated description of the database is presented in Table 1.

Table 1: Details of the database

Description	Heart Statlog	Pima Indian Diabetes	EEG Eyestate
No. of instances	270	768	14980
No. of attributes	13	8	15
No. of class	2	2	2
No. of samples in class 1	150	268	82527
No. of samples in class 2	120	500	6723

The confusion matrices of the BAERDL-SHDDC algorithm on the three datasets are reported in Fig. 3. The outcomes demonstrate that the BAERDL-SHDDC system results in the effectual identification of two classes on the three datasets.

In Table 2, the simulation outcomes of the BAERDL-SHDDC methodology are tested on the Heart Statlog database. The outcomes showed proficient results of the BAERDL-SHDDC technique in both classes. On the complete database, the BAERDL-SHDDC system reaches an average $accu_{bal}$ of 97.83%, $prec_n$ of 97.68%, $reca_l$ of 97.83%, F_{score} of 97.75%, and MCC of 95.52%. Meanwhile, on 70% TRP, the BAERDL-SHDDC method reaches an average $accu_{bal}$ of 98.45%, $prec_n$ of 98.34%, $reca_l$ of 98.45%, F_{score} of 98.39%, and MCC of 96.80%.

Table 2: Classifier outcome of BAERDL-SHDDC method on Heart statlog database

Heart Statlog Dataset					
Class	Accuracybal	Precision	Recall	F-Score	MCC
Entire Dataset					
C-1	97.33	98.65	97.33	97.99	95.52
C-2	98.33	96.72	98.33	97.52	95.52
Average	97.83	97.68	97.83	97.75	95.52
Training Phase (70%)					
C-1	98.10	99.04	98.10	98.56	96.80
C-2	98.81	97.65	98.81	98.22	96.80
Average	98.45	98.34	98.45	98.39	96.80
Testing Phase (30%)					
C-1	95.56	97.73	95.56	96.63	92.55
C-2	97.22	94.59	97.22	95.89	92.55
Average	96.39	96.16	96.39	96.26	92.55

DOI: https://doi.org/10.54216/JCIM.150209
Received: May 05, 2024 Revised: July 10, 2024 Accepted: October 22, 2024

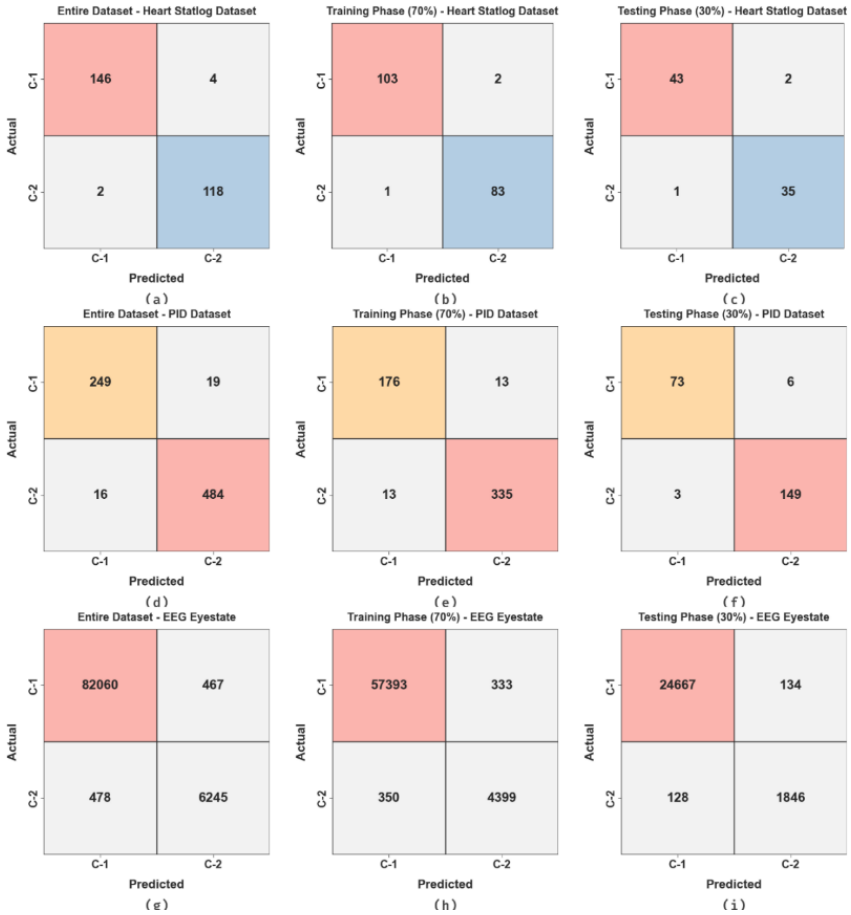

Figure 3. Confusion matrices of (a-c) Heart Statlog, (d-f) PID, and (g-i) EEG eyestate datasets

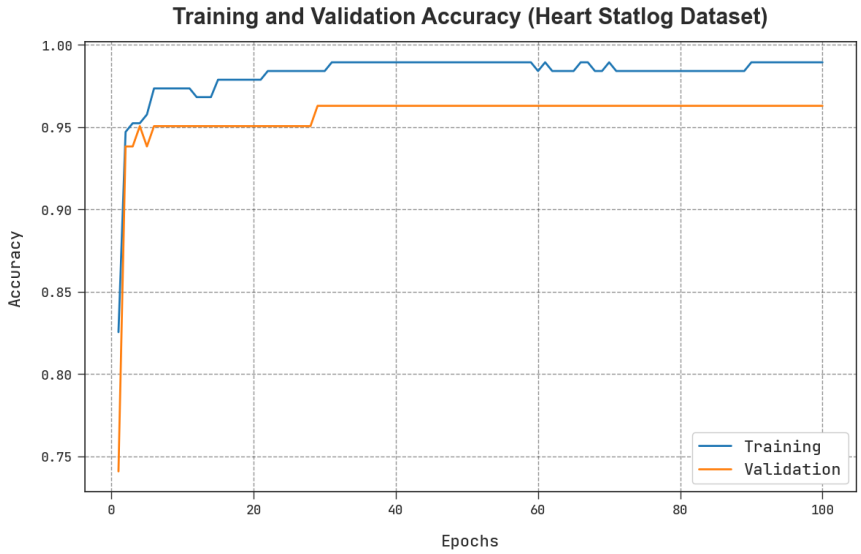

Figure 4. TACY and VACY outcomes of BAERDL-SHDDC system on Heart Statlog database

The TACY and VACY of the KELMCCP approach on the Heart Statlog dataset are represented in Fig. 4. The figure shows that the KELMCCP method has exposed improved performance with higher values of TACY and VACY. Visibly, the KELMCCP approach has reached maximum TACY results.

The TLOS and VLOS of the KELMCCP algorithm on the Heart Statlog dataset are signified in Fig. 5. The figure indicated that the KELMCCP methodology has superior performance with the least values of TLOS and VLOS. Especially, the KELMCCP technique has reduced VLOS results.

DOI: https://doi.org/10.54216/JCIM.150209
Received: May 05, 2024 Revised: July 10, 2024 Accepted: October 22, 2024

Figure 5. TLOS and VLOS outcomes of BAERDL-SHDDC system on Heart Statlog database

In Table 3, the outcomes of the BAERDL-SHDDC system are tested on the PID database. The results showed the proficient results of the BAERDL-SHDDC technique in both classes. On the complete database, the BAERDL-SHDDC approach reaches an average $accu_{bal}$ of 94.86%, $prec_n$ of 95.09%, $reca_l$ of 94.86%, F_{score} of 94.97%, and MCC of 89.95%. In the meantime, on 70% TRP, the BAERDL-SHDDC method reaches an average $accu_{bal}$ of 94.69%, $prec_n$ of 94.69%, $reca_l$ of 94.69%, F_{score} of 94.69%, and MCC of 89.39%.

Table 3: Classifier outcome of BAERDL-SHDDC method on PID dataset

Pima Indian Diabetes Dataset					
Class	Accuracybal	Precision	Recall	F-Score	MCC
Entire Dataset					
C-1	92.91	93.96	92.91	93.43	89.95
C-2	96.80	96.22	96.80	96.51	89.95
Average	94.86	95.09	94.86	94.97	89.95
Training Phase (70%)					
C-1	93.12	93.12	93.12	93.12	89.39
C-2	96.26	96.26	96.26	96.26	89.39
Average	94.69	94.69	94.69	94.69	89.39
Testing Phase (30%)					
C-1	92.41	96.05	92.41	94.19	91.30
C-2	98.03	96.13	98.03	97.07	91.30
Average	95.22	96.09	95.22	95.63	91.30

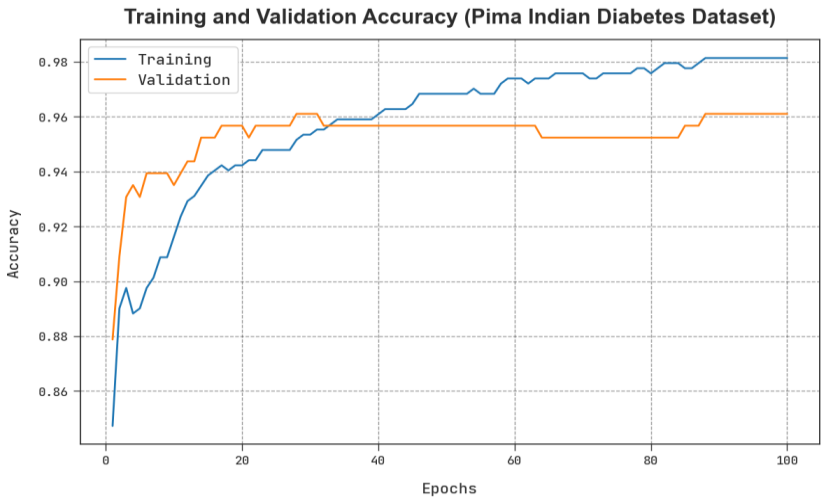

Figure 6. TACY and VACY outcomes of BAERDL-SHDDC system on PID dataset

DOI: https://doi.org/10.54216/JCIM.150209
Received: May 05, 2024 Revised: July 10, 2024 Accepted: October 22, 2024

The TACY and VACY of the KELMCCP system on the PID dataset are given in Fig. 6. The figure shows that the KELMCCP system has displayed superior performance with greater values of TACY and VACY. In particular, the KELMCCP algorithm has greater TACY results.

The TLOS and VLOS of the KELMCCP algorithm on the PID dataset are represented in Fig. 7. The figure exhibited that the KELMCCP model has exposed better performance with the least values of TLOS and VLOS. It is noticeable that the KELMCCP methodology has developed in lesser VLOS results.

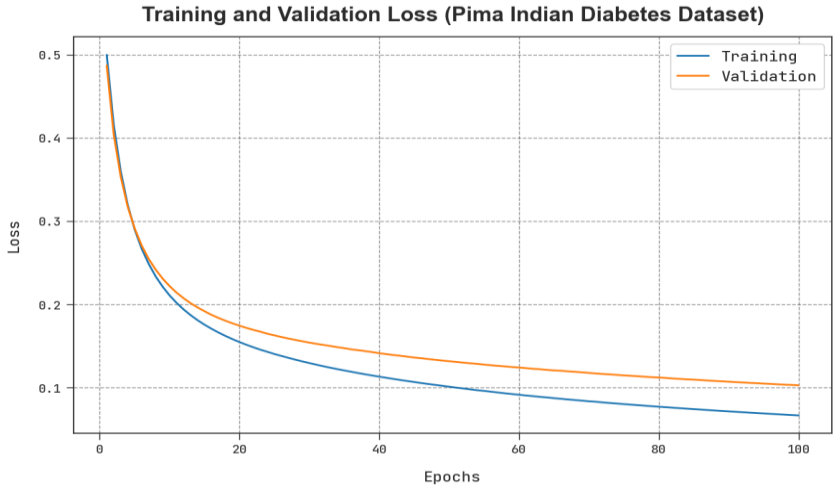

Figure 7. TLOS and VLOS outcomes of BAERDL-SHDDC model on PID dataset

In Table 4, the stimulation outcomes of the BAERDL-SHDDC model are tested on the EEG Eyestate dataset. The findings showed the proficient results of the BAERDL-SHDDC technique in both classes. On the entire dataset, the BAERDL-SHDDC approach reaches an average $accu_{bal}$ of 96.16%, $prec_n$ of 96.23%, $reca_l$ of 96.16%, F_{score} of 96.20%, and MCC of 92.39%. In the meantime, on 70% TRP, the BAERDL-SHDDC method reaches an average $accu_{bal}$ of 96.03%, $prec_n$ of 96.18%, $reca_l$ of 96.03%, F_{score} of 96.10%, and MCC of 92.20%.

Table 4: Classifier outcome of BAERDL-SHDDC method on EEG Eyestate dataset

EEG Eyestate					
Class	Accuracybal	Precision	Recall	F-Score	MCC
Entire Dataset					
C-1	99.43	99.42	99.43	99.43	92.39
C-2	92.89	93.04	92.89	92.97	92.39
Average	96.16	96.23	96.16	96.20	92.39
Training Phase (70%)					
C-1	99.42	99.39	99.42	99.41	92.20
C-2	92.63	92.96	92.63	92.80	92.20
Average	96.03	96.18	96.03	96.10	92.20
Testing Phase (30%)					
C-1	99.46	99.48	99.46	99.47	92.85
C-2	93.52	93.23	93.52	93.37	92.85
Average	96.49	96.36	96.49	96.42	92.85

The TACY and VACY of the KELMCCP model on the EEG Eyestate dataset are represented in Fig. 8. The figure shows that the KELMCCP model has presented greater performance with better values of TACY and VACY. In particular, the KELMCCP approach has maximal TACY results.

DOI: https://doi.org/10.54216/JCIM.150209
Received: May 05, 2024 Revised: July 10, 2024 Accepted: October 22, 2024

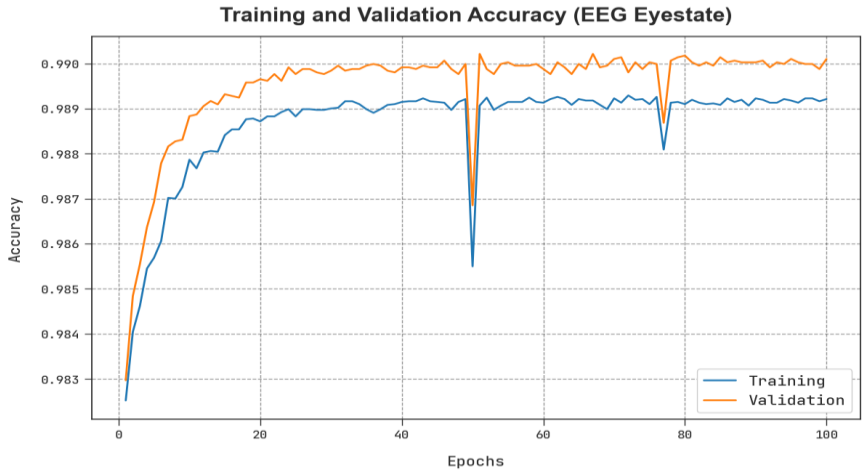

Figure 8. TACY and VACY outcomes of BAERDL-SHDDC system on EEG Eyestate dataset

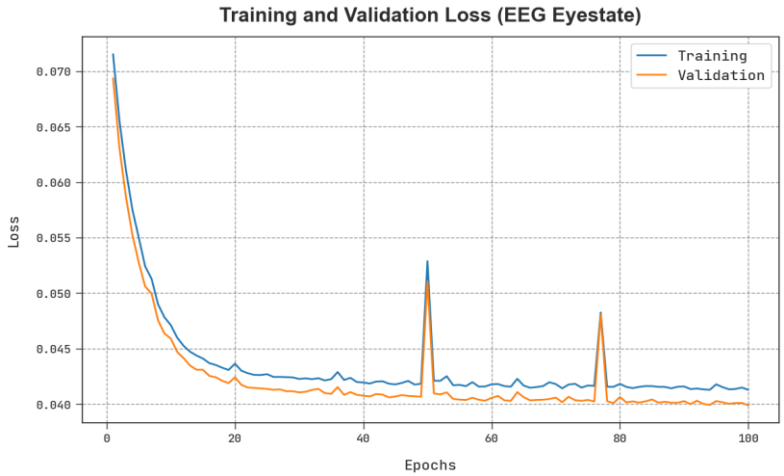

Figure 9. TLOS and VLOS outcomes of BAERDL-SHDDC system on EEG Eyestate database

The TLOS and VLOS of the KELMCCP technique on the EEG Eyestate dataset are denoted in Fig. 9. The figure displayed that the KELMCCP approach has superior performance with lesser values of TLOS and VLOS. Visibly, the KELMCCP method has the least VLOS results.

Table 5 and Fig. 10, comparison study of the BAERDL-SHDDC methods with current techniques on the heart Statlog database [23]. The outcomes report that the TR and RBF networks exhibit the least classifier outcomes. Then, the EEPSOC-ANN, DOD-GBT, and GBT models attain moderately closer classification performance. Next, the HBESDM-DLD technique results in reasonable performance with $an\ accu_y$ of 97.95%, $prec_n$ of 97.60%, $reca_l$ of 97.59%, and F_{score} of 97.76%. However, the BAERDL-SHDDC technique accomplishes superior performance with an $accu_y$ of 98.45%, $prec_n$ of 98.34%, $reca_l$ of 98.45%, and F_{score} of 98.39%.

Table 5: Comparative outcome of BAERDL-SHDDC model with other techniques on heart Statlog database

Heart Statlog Dataset				
Methods	$Accu_y$	$Prec_n$	$Reca_l$	F_{score}
BAERDL-SHDDC	98.45	98.34	98.45	98.39
HBESDM-DLD	97.95	97.60	97.59	97.76
EEPSOC-ANN	94.60	94.64	96.97	96.82
DOD-GBT	96.32	95.56	96.96	96.50
GBT	95.59	96.32	94.34	95.53
Random Tree	76.60	74.23	73.19	73.73
RBF Network	84.13	80.36	83.51	82.25

DOI: https://doi.org/10.54216/JCIM.150209
Received: May 05, 2024 Revised: July 10, 2024 Accepted: October 22, 2024

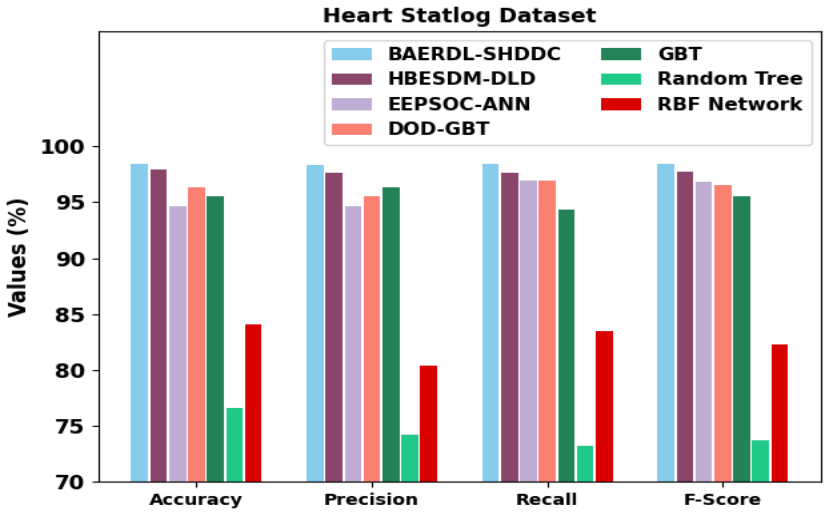

Figure 10. Comparative outcome of BAERDL-SHDDC system on heart Statlog data

In Table 6 and Fig. 11, a comparison study of the BAERDL-SHDDC method with current models on the PID dataset. The results report that the Logit-Boost and DT exhibit the least classifier outcomes. Then, the MR-OGBT, LR, and Voted Perceptron methods attain moderately closer classification performance. Following, the HBESDM-DLD technique results in reasonable performance with $accu_y$ of 94.65%, $prec_n$ of 93.94%, $reca_l$ of 94.66%, and F_{score} of 93.25%. But, the BAERDL-SHDDC technique accomplishes superior performance with $accu_y$ of 95.22%, $prec_n$ of 96.09%, $reca_l$ of 95.22%, and F_{score} of 95.63%.

Table 6: Comparative outcome of BAERDL-SHDDC model with other systems on PID database

Pima Indian Diabetes Dataset				
Methods	$Accu_y$	$Prec_n$	$Reca_l$	F_{score}
BAERDL-SHDDC	95.22	96.09	95.22	95.63
HBESDM-DLD	94.65	93.94	94.66	93.25
MR-OGBT	89.31	92.37	90.69	91.15
LR	77.42	87.73	78.98	83.54
Voted Perceptron	66.74	92.00	67.94	78.01
Logit-Boost	74.00	85.32	78.29	81.23
DT	74.26	80.98	78.76	80.55

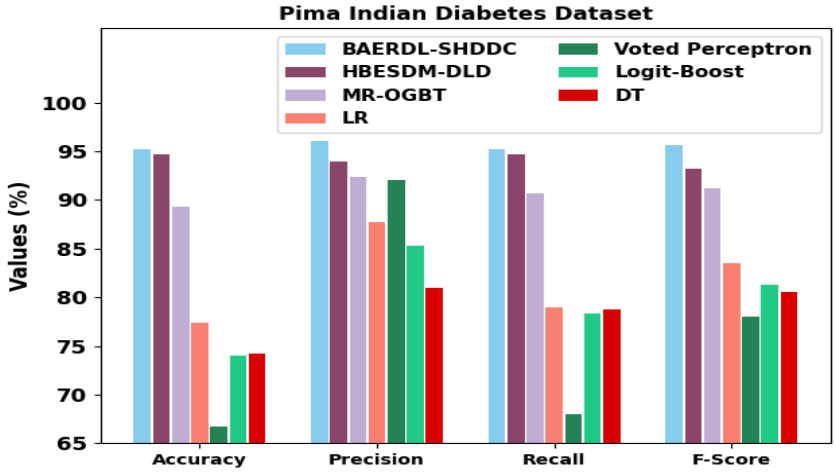

Figure 11. Comparative outcome of BAERDL-SHDDC model on PID database

DOI: https://doi.org/10.54216/JCIM.150209
Received: May 05, 2024 Revised: July 10, 2024 Accepted: October 22, 2024

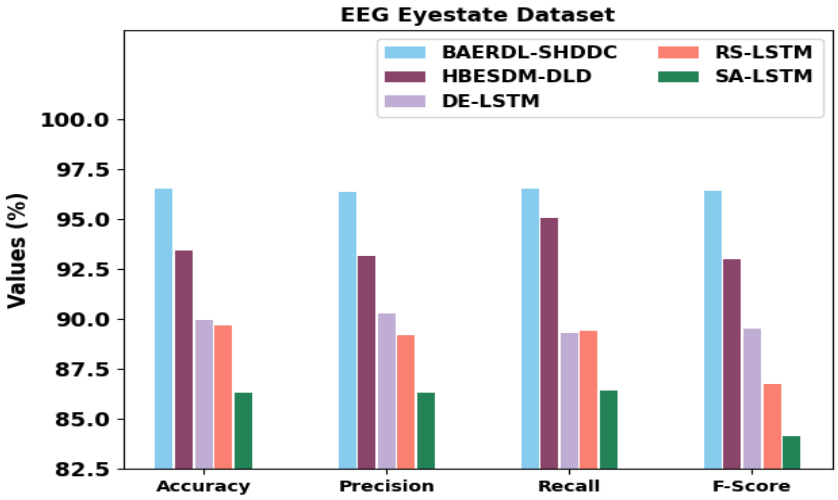

Figure 12. Comparative outcome of BAERDL-SHDDC approach on EEG Eyestate dataset

In Table 7 and Fig. 12, a clear comparison study of the BAERDL-SHDDC algorithm with current approaches on the EEG Eyestate dataset. The values report that the SA-LSTM shows the least classifier outcomes. Then, the DE-LSTM and RS-LSTM methods achieve moderately closer classification performance. Next, the HBESDM-DLD method results in reasonable performance with $accu_y$ of 93.40%, $prec_n$ of 93.12%, $reca_l$ of 95.03%, and F_{score} of 92.98%. However, the BAERDL-SHDDC method accomplishes superior performance with $accu_y$ of 96.49%, $prec_n$ of 96.36%, $reca_l$ of 96.49%, and F_{score} of 96.42%.

Table 7: Comparative outcome of BAERDL-SHDDC model with other models on EEG Eyestate database

EEG Eyestate Dataset				
Methods	$Accu_y$	$Prec_n$	$Reca_l$	F_{score}
BAERDL-SHDDC	96.49	96.36	96.49	96.42
HBESDM-DLD	93.40	93.12	95.03	92.98
DE-LSTM	89.97	90.29	89.29	89.51
RS-LSTM	89.67	89.21	89.38	86.74
SA-LSTM	86.30	86.30	86.42	84.13

These result analyses reassured the enhancements of the BAERDL-SHDDC technique on the disease classification process.

5. Conclusion

In this study, we have proposed a novel BAERDL-SHDDC method for sustainable and secure healthcare management. The presented BAERDL-SHDDC technique exploited BC technology for secure patient data management and DL models to examine the data for the disease detection process. The BAERDL-SHDDC technique offered improved security for patient data with enhanced disease classification performance via feature selection and ensemble process. For disease detection, the BAERDL-SHDDC technique involves a three-stage process namely AER-based feature selection, ensemble DL classification, and parameter optimization. The hyperparameters of the ensemble DL models are optimally selected by the use of an Adadelta optimizer. The stimulated result study of the BAERDL-SHDDC model shows the promising performance over other current techniques with greater accuracy of 98.45%, 95.22%, and 96.49% under Heart Statlog, Pima Indian Diabetes, and EEG Eyestate datasets respectively. The application of AER-based feature selection, ensemble model, and Adadelta optimizer assist in accomplishing enhanced detection results of the proposed model. Limitations of the BAERDL-SHDDC technique arise from challenges in scalability and resource usage, stemming from the combination of Deep Learning and Blockchain. Additionally, further validation on diverse datasets and real-world healthcare scenarios is necessary. In the future, the performance of the presented technique is developed by metaheuristic-based hyperparameter optimization techniques. In addition, the computational difficulty of the presented method needs to be investigated in the future.

DOI: https://doi.org/10.54216/JCIM.150209
Received: May 05, 2024 Revised: July 10, 2024 Accepted: October 22, 2024

Funding: "The author extends his appreciation to the Arab Open University for funding this work through AOU research fund No. (AOUKSA524008)"

Conflicts of Interest: "The authors declare no conflict of interest."

References

[1] Jain, S., Anand, A., Gupta, A., Awasthi, K., Gujrati, S. and Channegowda, J., 2020, February. Blockchain and Machine Learning in Health Care and Management. In 2020 International Conference on Mainstreaming Block Chain Implementation (ICOMBI) (pp. 1-5). IEEE.

[2] Vyas, S., Gupta, M. and Yadav, R., 2019, February. Converging blockchain and machine learning for healthcare. In 2019 Amity International Conference on Artificial Intelligence (AICAI) (pp. 709-711). IEEE.

[3] Arza, M.S. and Panda, S.K., 2022. An Integration of Blockchain and Machine Learning into the Health Care System. In Machine Learning Adoption in Blockchain-Based Intelligent Manufacturing (pp. 33-58). CRC Press.

[4] Maseleno, A., Hashim, W., Perumal, E., Ilayaraja, M. and Shankar, K., 2020. Access control and classifier-based blockchain technology in e-healthcare applications. In Intelligent Data Security Solutions for e-Health Applications (pp. 151-167). Academic Press.

[5] Mallikarjuna, B., Shrivastava, G. and Sharma, M., 2022. Blockchain technology: A DNN token-based approach in healthcare and COVID-19 to generate extracted data. Expert Systems, 39(3), p.e12778.

[6] Pardakhe, N.V. and Deshmukh, V.M., 2019, December. Machine learning and blockchain techniques used in healthcare system. In 2019 IEEE Pune Section International Conference (PuneCon) (pp. 1-5). IEEE.

[7] Das, S., Das, J., Modak, S. and Mazumdar, K., 2022. Internet of Things with Machine Learning-Based Smart Cardiovascular Disease Classifier for Healthcare in Secure Platform. In Internet of Things and Data Mining for Modern Engineering and Healthcare Applications (pp. 45-64). Chapman and Hall/CRC.

[8] Kim, S.K. and Huh, J.H., 2020. Artificial neural network blockchain techniques for healthcare system: Focusing on the personal health records. Electronics, 9(5), p.763.

[9] UmaMaheswaran, S.K., Prasad, G., Omarov, B., Abdul-Zahra, D.S., Vashistha, P., Pant, B. and Kaliyaperumal, K., 2022. Major Challenges and Future Approaches in the Employment of Blockchain and Machine Learning Techniques in the Health and Medicine. Security and Communication Networks, 2022.

[10] Li, Y., Shan, B., Li, B., Liu, X. and Pu, Y., 2021. Literature review on the applications of machine learning and blockchain technology in smart healthcare industry: a bibliometric analysis. Journal of Healthcare Engineering, 2021.

[11] Veeramakali, T., Siva, R., Sivakumar, B., Senthil Mahesh, P.C. and Krishnaraj, N., 2021. An intelligent internet of things-based secure healthcare framework using blockchain technology with an optimal deep learning model. The Journal of Supercomputing, pp.1-21.

[12] Neelakandan, S., Beulah, J.R., Prathiba, L., Murthy, G.L.N., Irudaya Raj, E.F. and Arulkumar, N., 2022. Blockchain with deep learning-enabled secure healthcare data transmission and diagnostic model. International Journal of Modeling, Simulation, and Scientific Computing, 13(04), p.2241006.

[13] Nguyen, G.N., Le Viet, N.H., Elhoseny, M., Shankar, K., Gupta, B.B. and Abd El-Latif, A.A., 2021. Secure blockchain enabled Cyber–physical systems in healthcare using deep belief network with ResNet model. Journal of parallel and distributed computing, 153, pp.150-160.

[14] Chen, M., Malook, T., Rehman, A.U., Muhammad, Y., Alshehri, M.D., Akbar, A., Bilal, M. and Khan, M.A., 2021. Blockchain-Enabled healthcare system for detection of diabetes. Journal of Information Security and Applications, 58, p.102771.

[15] Ashraf, E., Areed, N.F., Salem, H., Abdelhay, E.H. and Farouk, A., 2022, June. Fidchain: Federated intrusion detection system for blockchain-enabled iot healthcare applications. In Healthcare (Vol. 10, No. 6, p. 1110). MDPI.

[16] Smahi, A., Xia, Q., Gao, J. and Xia, H., 2021, March. An efficient and secure blockchain-based SVM classification for a COVID-19 healthcare system. In 2021 6th International Conference on Mathematics and Artificial Intelligence (pp. 122-129).

[17] Bi, H., Liu, J. and Kato, N., 2021. Deep learning-based privacy preservation and data analytics for IoT enabled healthcare. IEEE Transactions on Industrial Informatics, 18(7), pp.4798-4807.

[18] Antwi, M., Adnane, A., Ahmad, F., Hussain, R., ur Rehman, M.H. and Kerrache, C.A., 2021. The case of HyperLedger Fabric as a blockchain solution for healthcare applications. Blockchain: Research and Applications, 2(1), p.100012.

DOI: https://doi.org/10.54216/JCIM.150209
Received: May 05, 2024 Revised: July 10, 2024 Accepted: October 22, 2024

[19] Abdelhamid, A.A., El-Kenawy, E.S.M., Khodadadi, N., Mirjalili, S., Khafaga, D.S., Alharbi, A.H., Ibrahim, A., Eid, M.M. and SaAER, M., 2022. Classification of monkeypox images based on transfer learning and the Al-Biruni Earth Radius Optimization algorithm. Mathematics, 10(19), p.3614.

[20] Zhao, X., Lv, H., Wei, Y., Lv, S. and Zhu, X., 2021. Streamflow forecasting via two types of predictive structure-based gated recurrent unit models. Water, 13(1), p.91.

[21] Kim, D., Kwon, D., Park, L., Kim, J. and Cho, S., 2020. Multiscale LSTM-based deep learning for very-short-term photovoltaic power generation forecasting in smart city energy management. IEEE Systems Journal, 15(1), pp.346-354.

[22] Haji, S.H. and Abdulazeez, A.M., 2021. Comparison of optimization techniques based on gradient descent algorithm: A review. PalArch's Journal of Archaeology of Egypt/Egyptology, 18(4), pp.2715-2743.

[23] Sammeta, N. and Parthiban, L., 2022. Hyperledger blockchain enabled secure medical record management with deep learning-based diagnosis model. Complex & Intelligent Systems, 8(1), pp.625-640.

[24] https://archive.ics.uci.edu/dataset/264/eeg+eye+state

[25] https://www.kaggle.com/datasets/uciml/pima-indians-diabetes-database

[26] https://archive.ics.uci.edu/dataset/145/statlog+heart

DOI: https://doi.org/10.54216/JCIM.150209
Received: May 05, 2024 Revised: July 10, 2024 Accepted: October 22, 2024